Dynamic light scattering by nonergodic media: Brownian particles trapped in polyacrylamide gels

Jacques G. H. Joosten and Erik T. F. Geladé

Department for Physical and Analytical Chemistry, DSM Research, P.O. Box 18, 6160 MD Geleen, The Netherlands

Peter N. Pusey

Royal Signals and Radar Establishment, St. Andrews Road, Malvern WR14 3PS, England

(Received 12 March 1990)

Dynamic light scattering (DLS) is used to study the diffusional behavior of polystyrene latex spheres incorporated in polyacrylamide gels. It is shown that the gel systems exhibit nonergodic features, implying that the time-averaged intensity correlation function (ICF), the quantity obtained from a single DLS experiment, is not equal to the ensemble-averaged ICF. It is demonstrated that the theory of Pusey and van Megen [P. N. Pusey and W. van Megen, Physica A **157**, 705 (1989)] on DLS by nonergodic media can be used to extract dynamic structure factors from single DLS experiments. It appears from this analysis that large values of the diffusion coefficient of the tracer particles, which would have been obtained in a classical analysis, do not imply rapid particle motions but result simply from an incorrect analysis of the data. The initial decay of the dynamic structure factor gives a short-time diffusion coefficient of the particles that hardly depends on the degree of cross-linking. We also show that a proper analysis of the data results in a dynamic structure factor that develops a nondecaying component. This component is a measure for the fraction of frozen-in fluctuations resulting from constrained diffusion of the tracer particles. From the nondecaying component in the dynamic structure factor, a distribution of root-mean-square displacements of the particles is calculated that appears to be an exponential distribution of which the decay length decreases with increasing degree of cross-linking. Although the scattering from the systems with probes is much higher than that of the matrix, we cannot neglect the gel scattering completely. We present theoretical expressions allowing corrections for gel scattering.

I. INTRODUCTION

In recent years the characterization of polymeric gels by measuring the diffusional behavior of probe particles, which are dispersed in the gel system, has attracted a great deal of attention.[1-4] A related approach can be used to study certain features of the glass transition in colloidal glasses.[5] Also the problem of estimating the validity of various expressions modeling the transport properties of large spheres in concentrated polymer solutions has been studied extensively.[6-9]

Ideally, a polymeric gel is thought to consist of a three-dimensional random collection of polymer coils having their ends chemically connected to cross-links. Aqueous polyacrylamide gels resulting from a copolymerization of acrylamide with the cross-linking agent bisacrylamide and networks formed by copolymerization of styrene with a small amount of divinylbenzene are typical examples of such systems. Semidilute polymer solutions can be envisaged as transient statistical networks formed by the entanglement of polymer chains. For these systems it is possible to identify a characteristic correlation length ξ that describes the average distance between entanglement points.[10]

The basic idea behind these tracer studies is that the mobility of a particle incorporated in these systems depends on, among other things, the relative value of the size of the particle, d, and on the correlation length ξ of the network. Therefore, by measuring the mobility of particles of various sizes, one is able to obtain information on the morphology of the three-dimensional network.

Dynamic light scattering (DLS) is a well-suited technique for studying the movement of tracer particles in polymer solutions and gels. In a DLS experiment one determines the (normalized) time correlation function $g^{(2)}(q,\tau)$ of the scattered intensity which, under conditions to be discussed below, is given by[11]

$$g^{(2)}(q,\tau) = \langle I(q,0)I(q,\tau) \rangle / \langle I(q,0) \rangle^2$$
$$= 1 + |\beta f(q,\tau)|^2 , \tag{1}$$

where τ denotes time, and $I(q,\tau)$ is the scattered intensity at the scattering vector q: $q = (4\pi/\lambda)\sin(\Theta/2)$, with λ and Θ being the wavelength of the light and the scattering angle in the medium, respectively, and $f(q,\tau)$ the normalized intermediate scattering function. The so-called coherence factor β (≤ 1) in Eq. (1) depends on the experimental setup. Theoretically, the angular brackets in (1) denote an ensemble average, but in most practical situations the intensity-correlation-function data are taken from a correlator which replaces the ensemble average with a time average. This procedure is justified by invoking the ergodicity theorem.[11] Moreover expressing $g^{(2)}(q,\tau)$ as $1 + |\beta f(q,\tau)|^2$ (Siegert relation) only holds for scattering processes in which the scattered field is a zero-mean complex Gaussian variable.[12]

In simple cases $f(q,\tau)$ can be expressed as[13]

$$f(q,\tau) = e^{-\Gamma\tau} \, , \tag{2}$$

where Γ is the decay rate for the qth Fourier mode of concentration fluctuation given by

$$\Gamma = Dq^2 \, . \tag{3}$$

The parameter D is the diffusivity, which is the relevant physical quantity that is obtained from DLS experiments.

Recently, Pusey and van Megen[14] pointed out that for solidlike systems, like gels, Eq. (1) does not apply. The complications are caused by the fact that scatterers in a polymer gel are localized near fixed average positions and are able only to execute limited Brownian motions about these positions. By virtue of this localization of the scatterers, one sample of such a so-called nonergodic system will be trapped in a restricted region of phase space, or subensemble, whose location and extent are determined, respectively, by the average positions of the scatterers and the magnitude of their displacements. This case has to be contrasted to the situation occurring in a system in which the particles are able to diffuse throughout the whole sample, and therefore, given enough time, the system evolves through a representative fraction of all possible spatial configurations. This implies that such a system during a single experiment can explore enough of phase space so that the time average, inherent in the measurement of a property, gives a good estimate of its ensemble average. Usually the equivalence between time-averaged and ensemble-averaged time correlation functions is tacitly assumed, but for DLS experiments on gel systems the validity of this assumption has to be questioned. On the contrary, it appears that the complications caused by nonergodicity of the medium in a DLS experiment (that is, the nonequivalence of time and ensemble averages) have not been fully appreciated. We are only aware of the papers by Carlson and Fraser[1] and Sellen,[15] who have recognized some of the problems associated with DLS by nonergodic media.

The purpose of this paper is to present systematic DLS experiments on linear and cross-linked polyacrylamide gels in which we dispersed polystyrene spheres as tracer particles.

The objectives of our study are to use and check the theory of DLS by nonergodic media, which was put forward by Pusey and van Megen,[14] and thereby to obtain information on the morphology of the gel systems.

The paper is organized as follows: In Sec. II the relevant notions and equations from Ref. 14 will be recapitulated and elaborated. Section III deals with the experimental details, and here we present some experimental results on systems that are obtained by copolymerizing acrylamide and bisacrylamide. The total monomer content of the gels is kept constant at 2.5 wt. %, whereas the cross-link content is varied. The tracer particles have a diameter of about 85 nm, and the concentration of the spheres is 2×10^{-2} wt. %. Section IV is devoted to a discussion of the results in view of the theory of DLS by nonergodic media. We find that the gels under study indeed show the nonergodic behavior and that the experimental results can be interpreted reasonably well by the theory formulated in Ref. 14.

II. THEORETICAL BACKGROUND

For a proper understanding of the equations used in the interpretation of the experimental data, we will summarize the notions and expressions pertinent to DLS experiments by nonergodic media in this section. Full details can be found in the paper by Pusey and van Megen.[14]

We consider a medium that contains discrete scatterers (particles) for which the instantaneous field amplitude of the light scattered by N particles in a scattering volume V is given by

$$E(q,\tau) = \sum_{j=1}^{N} b_j \exp[i\mathbf{q}\cdot\mathbf{r}_j(\tau)] \, , \tag{4}$$

and the intermediate scattering function (or dynamic structure factor) is defined by[13]

$$F(q,\tau)$$
$$= (Nb^2)^{-1} \sum_{j=1}^{N} \sum_{k=1}^{N} \langle b_j b_k \exp\{i\mathbf{q}\cdot[\mathbf{r}_j(0) - \mathbf{r}_k(\tau)]\} \rangle_E \, , \tag{5}$$

where $b_i = b_i(q)$ is the field amplitude of the light scattered by particle i at scattering vector $\mathbf{q}$ and $\mathbf{r}_i(\tau)$ is the position of the center of mass of particle i at time τ. The subscript E in (5) emphasizes that the average (denoted by the angular brackets) has to be taken over the full ensemble.

The ensemble-averaged scattered intensity is given by

$$\langle I(q) \rangle_E = \sum_{j=1}^{N} \sum_{k=1}^{N} \langle b_j b_k \exp[i\mathbf{q}\cdot(\mathbf{r}_j - \mathbf{r}_k)] \rangle_E \, ,$$
$$= Nb^2 F(q,0) \, , \tag{6}$$

where $F(q,0)$ is the usual static structure factor, and $Nb^2 F(q,\tau)$ can be identified as the ensemble-averaged time correlation function of the scattered field amplitude.[13]

We also define a normalized dynamic structure factor $f(q,\tau)$ by

$$f(q,\tau) = F(q,\tau)/F(q,0) \tag{7}$$

and a normalized ensemble-averaged intensity correlation function (ICF) by

$$g_E^{(2)}(q,\tau) = \langle I(q,0)I(q,\tau) \rangle_E / \langle I(q,0) \rangle_E^2$$
$$= 1 + |f(q,\tau)|^2 \, . \tag{8}$$

Comparing the latter equation with (1), one notices the absence of the factor β in (8). The reason for this is that (8) applies to the intensity scattered to a single point in the far field. In practice, however, the exposed area of the detector is finite, and account must be taken of this particle spatial coherence resulting in $\beta < 1$. In the presentation of the theoretical equations, we always take $\beta = 1$.

Next to the ensemble-averaged intensity and ICF, we have to deal with the corresponding time-averaged quantities [$\langle I(q) \rangle_T$ and $g_T^{(2)}(q,\tau)$, respectively] because, in

general, these quantities will be determined in an actual experiment. For ergodic media there exists, by definition, an equivalence between time and ensemble averages, so that Eq. (8) can be used directly for extracting $f(q,\tau)$ from experimental ICF's.

We now focus attention on a nonergodic medium by first noting that the light scattered by a particular scattering volume of such a system constitutes a speckled pattern composed of both fluctuating and nonfluctuating components. At any point in the far field, the intensity will undergo restricted fluctuations about a mean value, which itself will vary from point to point and be determined by the average positions of the scatterers in the particular scattering volume under study. Now, time and ensemble averages will, in general, be different.

Faced with a nonergodic medium of interest, one has two choices. The first is to construct the ensemble-averaged ICF by moving the sample through a series of positions so that different scattering volumes within the sample are illuminated. At each position an ICF of the scattered light is measured, and finally the ensemble average is evaluated. After this tedious procedure, the ensemble-averaged dynamic structure factor $f(q,\tau)$ can then be obtained in the usual way, i.e., using Eq. (1). Pusey and van Megen worked out the alternative procedure; i.e., they calculated directly the scattering properties of a single scattering volume in the nonergodic medium and used this in order to obtain $f(q,\tau)$ from a single ICF measurement.

The model starts off by noticing that the total scattered field (4) in a nonergodic medium is not a zero-mean complex Gaussian variable since, because of the spatial restrictions of the scatterers, the phase factors $\{\mathbf{q}\cdot\mathbf{r}_i(\tau)\}$ do not in time undergo fluctuations large compared with 2π. Nonergodicity of the medium is modeled by allowing only limited excursions $\{\Delta_j\}$ of the particles about their fixed average positions $\{R_j\}$. This is expressed in the center-of-mass position of a particle:

$$r_j(\tau)=R_j+\Delta_j(\tau) \ ,$$

where

$$R_j=\langle r_j(\tau)\rangle_T, \quad \langle\Delta_j(\tau)\rangle_T=0 \ . \tag{9}$$

Then, the total scattered field is written as the sum of fluctuating component $E_F(q,\tau)$ and a time-independent component $E_C(q)$:

$$E(q,\tau)=E_F(q,\tau)+E_C(q) \ . \tag{10}$$

The basic difference between DLS by ergodic media and DLS by nonergodic media is illustrated by the observation that the ensemble average of $E(q,\tau)$ is zero and that its time average is nonzero and can be written as

$$\langle E(q)\rangle_T=E_C(q) \ .$$

The time average of the total scattered intensity can be expressed as

$$\langle I(q)\rangle_T=\langle|E(q,\tau)|^2\rangle_T \ ,$$

$$=\langle I_F(q)\rangle_T+I_C(q) \ . \tag{11}$$

The time-averaged statistical properties of the fluctuating component $E_F(q,\tau)$ of the field scattered by a particular volume of the sample can be written in terms of full ensemble averages of the system;[14] i.e.,

$$\langle E_F(q,0)E_F^*(q,\tau)\rangle_T=\langle I(q)\rangle_E[f(q,\tau)-f(q,\infty)] \ , \tag{12}$$

and

$$\langle I_F(q)\rangle_T=\langle I(q)\rangle_E[1-f(q,\infty)] \ , \tag{13}$$

where $f(q,\infty)$ is the limiting value of $f(q,\tau)$ for $\tau\to\infty$, and (13) follows from (12) by taking the $\tau=0$ limit. Nonergodicity of the medium enters the problem only through the constant component $E_C(q)$, which depends explicitly on the relevant configuration of the scatterers $\{R_j\}$ and will therefore be different for different scattering volumes.

Calculation of the time-averaged ICF associated with the field (10) is now accomplished by our noting that it is equivalent to the usual heterodyne situation, where a Gaussian and a constant field are mixed. This leads to

$$\langle I(q,0)I(q,\tau)\rangle_T-\langle I(q,0)\rangle_T^2$$

$$=\langle I(q)\rangle_E^2[f(q,\tau)-f(q,\infty)]^2$$

$$+2I_C(q)\langle I(q)\rangle_E[f(q,\tau)-f(q,\infty)] \ . \tag{14}$$

In this equation, in the first term on the right-hand side, one recognizes the homodyne contribution, whereas the second term constitutes the heterodyne part to the total ICF. Now using (11) and (13) for expressing $I_C(q)$ in $\langle I(q)\rangle_T$ and $\langle I(q)\rangle_E$, (14) can be written as

$$g_T^{(2)}(q,\tau)=\langle I(q,0)I(q,\tau)\rangle_T/\langle I(q,0)\rangle_T^2$$

$$=1+Y^2[f^2(q,\tau)-f^2(q,\infty)]$$

$$+2Y(1-Y)[f(q,\tau)-f(q,\infty)] \ , \tag{15}$$

where

$$Y=\langle I(q)\rangle_E/\langle I(q)\rangle_T \ . \tag{16}$$

Equations (15) and (16) will be used for extracting the dynamic structure factor $f(q,\tau)$ from DLS data.

We will now briefly discuss a few general features of Eq. (15). First, as one notices from this equation, the time-averaged ICF is largely expressed in terms of ensemble-averaged quantities, but it still depends on the time-averaged intensity $\langle I(q)\rangle_T$ which itself depends explicitly on the configuration $\{R_j\}$ of fixed average positions of the particles in the particular volume under study. We also observe that for a fully fluctuating medium, i.e., an ergodic medium, for which $Y=1$ and $f(q,\infty)=0$, Eq. (15) reduces to the usual expression [see Eq. (8)]. For a partially fluctuating medium, i.e., a nonergodic medium, $f(q,\tau)$ starts at 1 and decays to constant nonzero value, $f(q,\infty)$, which provides a measure of that fraction of the number-density (or strictly refractive index) fluctuations which is frozen in. It is obvious that for analyzing a particular light-scattering experiment, it is still necessary to construct a theoretical model for the dynamic structure factor $f(q,\tau)$. This may be a formidable task for the gels, which will not be carried out here, but

we merely confine our discussion to some general features of experimental $f(q,\tau)$'s, such as its initial decay (first cumulant) and its value for long times $[f(q,\infty)]$.

To conclude this section, we present a few expressions that can be found from Eq. (15). The quadratic equation (15) can be solved for $f(q,\tau)$ and then used to calculate this quantity from the experimentally measured $g_T^{(2)}(q,\tau)$ and the value found for Y. This solution is

$$f(q,\tau)=(Y-1)/Y+[g_T^{(2)}(q,\tau)-\sigma_I^2]^{1/2}/Y , \quad (17)$$

where the mean-square intensity fluctuation σ_I^2 is given by

$$\sigma_I^2=\langle I^2(q)\rangle_T/\langle I(q)\rangle_T^2-1 . \quad (18)$$

The quantity σ_I^2 is experimentally accessible, because it represents the reduction of the initial amplitude of the measured ICF [i.e., $g_T^{(2)}(q,0)$] when compared with the ideal situation [i.e., an ergodic medium and $\beta=1$ in (1)]; σ_I^2 is related to $f(q,\infty)$ by

$$f(q,\infty)=(Y-1)/Y+(1-\sigma_I^2)^{1/2}/Y . \quad (19)$$

For a fully fluctuating medium, $\sigma_I^2=1$ and $Y=1$, and thus $f(q,\infty)=0$.

Finally, we give a short-time expansion of $g_T^{(2)}(q,\tau)$ that will be used to perform a cumulant analysis[16] of the ICF's. We start with a short-time expansion of the dynamic structure factor:

$$f(q,\tau)\approx 1-Dq^2\tau+\cdots , \quad (20)$$

where, in general, $D=D(q)$ is a diffusion coefficient. In the case emphasized in this paper, of independent tracer particles in gels, D can be identified as the short-time diffusion coefficient.[13] Substitution of (20) into (15) gives

$$g_T^{(2)}(q,\tau)-1=\sigma_I^2(1-2D_Aq^2\tau+\cdots) , \quad (21)$$

where D_A is an apparent diffusion coefficient given by

$$D_A=DY/\sigma_I^2 . \quad (22)$$

III. EXPERIMENTAL SECTION

A. Materials

Polyacrylamide gels or solutions are made by copolymerizing acrylamide (AA) and bisacrylamide (BAA), using ammonium persulfate as the initiator and tetramethylethylenediamine (TEMED) as the activator, in cylindrical glass cells (diameter, 1 cm). All chemicals are ultragrade quality and are purchased from LKB-Produkter AB Sweden. A series of samples, with and without latex spheres, are prepared. The total monomer content ([AA]+[BAA]) in all the samples is 2.5 wt. % whereas the cross-link content ([BAA]/[AA]) is 0, 1.5, 1.8, 2.0, and 4 wt. %, respectively. For the samples, with tracer particles, a small amount of an aqueous solution containing fairly monodisperse polystyrene spheres (Duke Scientific, 2 wt. % solids; diameter, 82±5 nm) are added to the pregel mixture prior to the initiation of the polymerization. Based on the data, given by the supplier

of the latex particles, the volume fraction occupied by the probes in the samples is approximately 2×10^{-4} ($\approx6.9\times10^{11}$ particles/ml). Before putting into the optical cuvettes (volume ~2 ml) all solutions are carefully made dust free. Gelation occurs within about 30 min at room temperature, but the samples are only used after 24 hr.

B. Experimental setup and methods

Dynamic-light-scattering experiments were carried out on an ALV/SP-86 goniometer (ALV, Langen, FRG) using an Ar$^+$ laser operating in TEM$_{00}$ mode at an output power of 200 mW. The incident beam (wavelength in vacuo, $\lambda_0=514.5$ nm) is polarized vertically with respect to the scattering plane and is focused in the scattering cell by a lens (focal length, 200 mm). A Glan-Thomson prism is used for detecting only vertically polarized scattered light. Toluene is used as the index matching and temperature-controlling fluid. The optical detection unit consists of a slit (width, ≈0.3 mm) which is imaged in the scattering cell by a lens ($2f$-$2f$ configuration; magnification, ≈1). In front of the photomultiplier (EMI 9863), we have a pinhole (diameter, ≈50 μm), and the distance between the slit and the pinhole is chosen such that only the main Airy disk of a speckle in the far field is detected. This results in an experimental contrast of 0.92 [factor β given in Eq. (1) equals 0.958] in the ICF for all scattering angles between 30° and 150° when measured for a dilute latex suspension. We emphasize that having this high contrast in the ergodic case is a prerequisite for obtaining unambiguous dynamic structure factors in the nonergodic case, because otherwise the spatial integration effects on the detector become mixed with the nonergodicity effects[14] (both effects reduce the contrast of an ICF).

Intensity correlation functions are measured by an ALV-3000 multibit correlator (ALV, Langen, FRG). The correlator is either operated in linear mode or in a multiple-τ mode. In linear mode, a 1024-point ICF can be measured whereas, in a multiple-τ mode, $g_T^{(2)}(q,\tau)$ consists of 192 logarithmically spaced channels allowing a time span of nine decades in one run. In a multiple-τ mode, the correlator has the option of using a special monitor channel for accumulating the number of counts for each set of eight channels starting from channel 89. The contents of these monitor channels are used for the so-called symmetrical normalization.[17] This feature improves the quality of the data substantially, especially for large delay times. In linear mode we typically take ten runs, each a length of 60 sec, and in multiple-τ mode we take three runs, each a length of 15 min. Normalization of the ICF's is accomplished by using the total number of photon counts and the number of summations from the correlator for calculating the base line [i.e., $\langle I(q)\rangle_T^2$] in each run. The final $g_T^{(2)}(q,\tau)$, which is used as raw data for the analysis, is then obtained by averaging the results of various runs.

Correlation functions are taken at scattering angles $\Theta=30°$, 50°, 70°, 90°, 120°, and 150°. The experiments are carried out at a temperature of 18.5 °C. To conclude this paragraph, we describe the method for determining

$\langle I(q)\rangle_E$. This quantity is measured by steadily turning the cuvette with the sample in the light-scattering apparatus, thereby scanning many independent speckles across the detector. Averaging of the scattered light intensity, received by the photomultiplier during this procedure at a particular scattering angle, is accomplished by the averaging mechanism of the frequency counter that is used for measuring the scattered light intensity. We find that this procedure works well and $\langle I(q)\rangle_E$ can be measured with an accuracy of $\pm 3\%$.

C. Results

The nonergodic nature of the gel systems is immediately apparent from the following observations: Scanning through various positions in the sample shows that there is a tremendous variation in the time-averaged scattered intensity $\langle I(q)\rangle_T$, implying that we are observing different subensembles of the total system. This $\langle I(q)\rangle_T$ for a particular position (speckle, scattering volume) and fixed scattering angle remains constant for a long time, i.e., minutes for the loose gels (low cross-linking) and hours for the strong gels (high cross-linking). The phenomena just described occur in the systems with the particles, as well as in the systems without the probes. Uncross-linked gels do not show this feature; i.e., $\langle I(q)\rangle_T$ is the same for all scattering volumes and is equal to $\langle I(q)\rangle_E$. The variation of $\langle I(q)\rangle_T$ is depicted in Fig. 1, where a frequency plot of the time-averaged scattered light intensity, $P(\langle I(q)\rangle_T)$ versus $\langle I(q)\rangle_T$ is given. The data are obtained by measuring $\langle I(q)\rangle_T$ at various positions in the cell, thereby keeping the scattering angle constant at $\Theta=90°$. The data are obtained from about 370 measurements, and the histogram is constructed by grouping the data in intervals of 20×10^3 counts/sec. The results plotted in Fig. 1 represent an estimate of the probability distribution $P(I(q))$ of the scattered intensity, as given in Eq. (11), sampled over the full ensemble. This probability distribution function shows a cutoff at low intensities imposed by the contribution of the fluctuating component $\langle I_F(q)\rangle_T$. In addition to this, we expect a negative exponential part resulting from $I_C(q)$.[12] It is easy to show that the scattered intensity $I(q)$ has the following probability distribution function when sampled over the full ensemble:

$$P(I(q))=H(I(q)-I_0)[\langle I(q)\rangle_E-I_0]^{-1}$$

$$\times \exp\{-[I(q)-I_0]/[\langle I(q)\rangle_E-I_0]\}, \quad (23)$$

where $H(x)$ is the Heaviside function, and $I_0=\langle I_F(q)\rangle_T=\langle I_F(q)\rangle_E$. The solid line in Fig. 1 is a nonlinear least-squares fit of the function $P(I(q))$ to the data. One notices that the data are fairly well described by this function, which implies that the scattered field $E(q,\tau)$, associated with this intensity, is a zero-mean Gaussian stochastic variable[12] over the full ensemble. From the parameters used to construct the curve in Fig. 1, we find $I_0=20\times 10^3$ counts/sec and $\langle I(q)\rangle_E=191\times 10^3$ counts/sec; whereas the procedure, described in the last paragraph to obtain $\langle I(q)\rangle_E$ gives, 190×10^3 counts/sec. By using Eq. (13) and realizing that
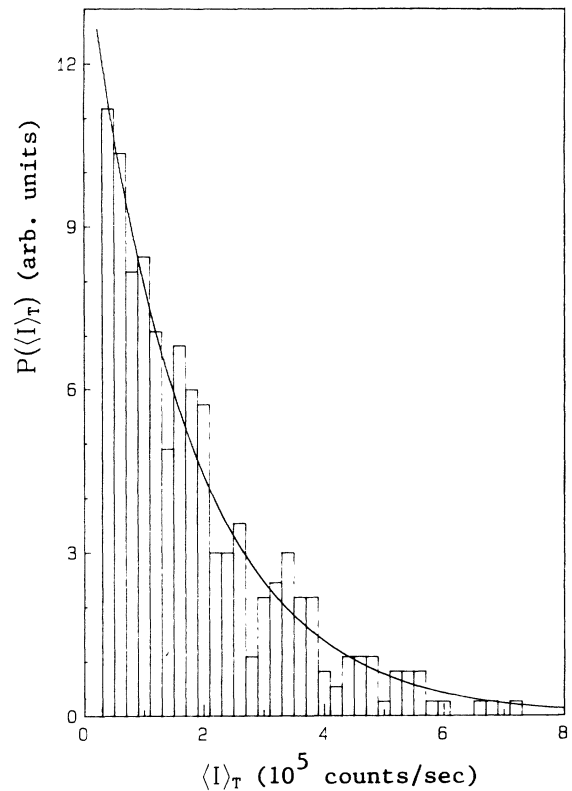

FIG. 1. Frequency distribution of $\langle I(q)\rangle_T$. Data taken from a gel ([BAA]/[AA]=2 wt. %) with tracer particles at a scattering angle of 90°. The solid line denotes the least-squares fit of Eq. (23) to the data, resulting in $I_0=\langle I_F(q)\rangle_T=\langle I_F(q)\rangle_E$ $=20\times 10^3$ counts/sec and $\langle I(q)\rangle_E=191\times 10^3$ counts/sec.

$\langle I_F(q)\rangle_T=\langle I_F(q)\rangle_E$, we find from these data that $f(q,\infty)=0.90$. This value agrees very well with the result we obtain for $f(q,\infty)$ from the analysis of time-averaged ICF's to be described below.

Because of the strong scattering from the tracer particles, their scattering intensity $\langle I(q)\rangle_E$ is measured to be at least 40 times larger than that of the pure polymer systems. In Fig. 2 we have plotted $\langle I(q)\rangle_E$ vs q for a gel system with particles. The solid line is found from a nonlinear least-squares fit to the data, using Mie theory[18] for the light scattering. As one can see, the fit is reasonably good, and a particle diameter of 83 nm is obtained when the index of refraction, n, for the particles is taken to be 1.59 and for the polymer solution it is measured to be 1.333.

We also measured the diffusion coefficient D_0 of a dispersion of latex particles in water at the same concentration as used in the polymer systems. The ICF's obtained for this sample show an essentially monoexponential behavior with a normalized second cumulant ≤ 0.05 for all angles. Furthermore, it appears that there is hardly any q dependence of D, and by applying the Stokes-Einstein relation we find a hydrodynamic diameter of 85 nm $[D_0=(4.8\pm 0.1)\times 10^{-12}$ m^2/sec]. Comparing now the results from static and dynamic-light-scattering experiments, we observe a reasonable agreement. Obvious-
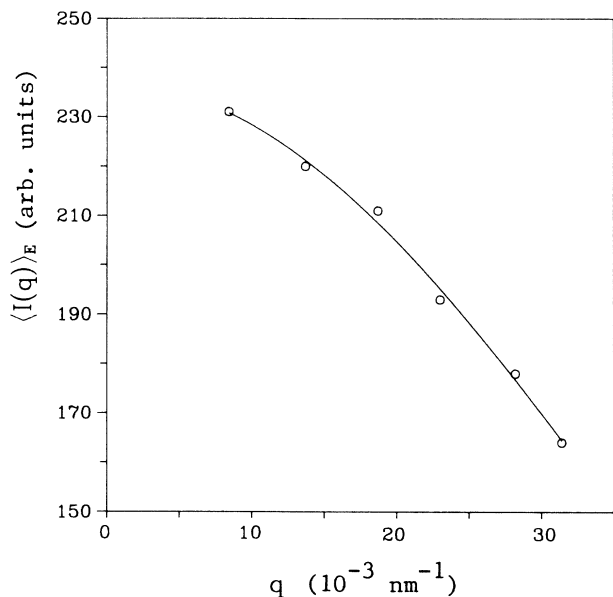
FIG. 2. Ensemble-averaged scattered light intensity $\langle I(q)\rangle_E$ vs scattering vector q (circles). Data taken from a gel ([BAA]/[AA]=4 wt. %) with polystyrene particles. Scattering angles are $\Theta=30°$, $50°$, $70°$, $90°$, $120°$, and $150°$. The solid line gives scattering according to Mie theory.

ly, the water dispersion is an ergodic system, and we used it on a regular basis for checking the light-scattering set-up and determining the coherence factor β.

Next we will present the results obtained for the un-cross-linked system ([BAA]/[AA]=0). In Fig. 3 a typical example of an ICF for this sample is shown. As can be
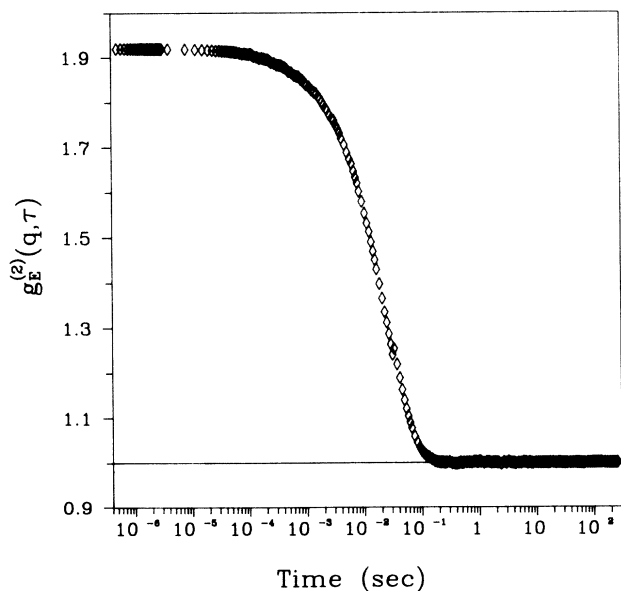
seen from the figure that the function has an amplitude of $1+\beta^2=1+(0.958)^2=1.92$ at $\tau=0$, and this means that this system exhibits ergodic characteristics. Therefore we may use Eq. (1) to find the intermediate scattering function $f(q,\tau)$. The result is given in Fig. 4. Analyzing this function shows that it does not have a monoexponential form but a fast decay at short times followed by a slower decay for longer times. The initial decay is quantified by applying a cumulant analysis[16] to the first part of $f(q,\tau)$ (τ varying from 0.5 to 120 μsec; the solid straight line in Fig. 4). Doing this for the functions measured at all angles between $30°$ and $150°$, it turns out that the diffusion coefficient, associated with this initial decay D is nearly q independent, and its value is found to be $D=(1.3\pm0.1)\times10^{-12}$ m^2/sec. The slow decay of the dynamic structure factors is determined by fitting a linear polynomial to the long-time part of the data (τ varying from 4 to 30 msec; the dashed straight line in Fig. 4). We also find that the decay constant of this long-time part scales very well with q^2, and for the diffusion coefficient of this slow process, D_L, we find a mean value of $(0.28\pm0.01)\times10^{-12}$ m^2/sec. If we now compare the ratio D_0/D_L (D_0 being the diffusion coefficient measured for the particles in water), we find that this ratio $(4.8/0.28=17)$ agrees very well with ratio of the macroscopic viscosities of these two media (the viscosity of the polymer solution was measured by means of an Ubbelohde viscosimeter, and we found a value of 17 mPa sec and that the viscosity of water at 18.5°C equals 1.04 mPa sec). The behavior found here is very similar to that found in concentrated colloidal dispersions,[13] where the short-time diffusion is mainly affected by hydrodynamic interactions and therefore reflects the local viscosity of

FIG. 3. Normalized intensity correlation function $g_T^{(2)}(q,\tau)=g_E^{(2)}(q,\tau)$ measured at $\theta=30°$ from the un-cross-linked polymer solution containing latex particles. Notice the amplitude of $g_T^{(2)}(q,\tau)$ for $\tau\to0$ indicating ergodic behavior. The solid line indicates the normalized base line.
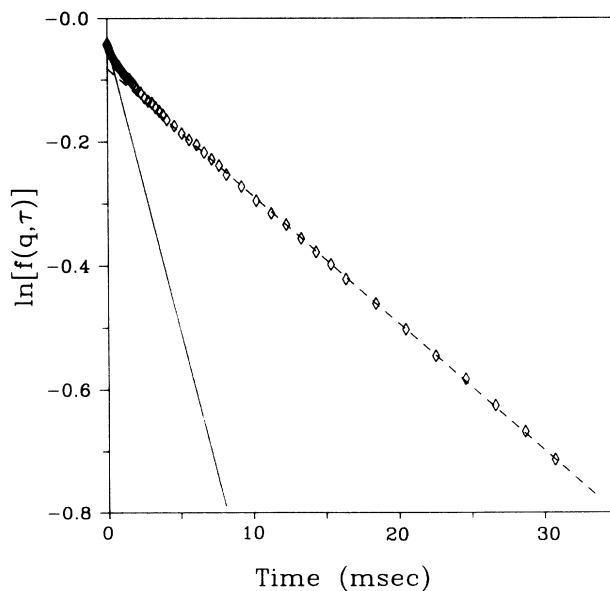

FIG. 4. The dynamic structure factor $f(q,\tau)$ obtained from $g_T^{(2)}(q,\tau)$ as plotted in Fig. 3 by using Eq. (1). Diamonds denote data points. The solid line is the result of a cumulant analysis of the initial decay, whereas the dashed line represents the long-time decay.

the environment in which a particle moves. The long-time diffusion is related to Brownian motion of the particles, in which direct and hydrodynamic interactions play a role, and therefore it is likely that this type of motion is affected by the macroscopic viscosity.

We now turn to the results achieved for the cross-linked gels containing tracer particles. In Fig. 5 we have plotted some typical examples of the normalized time-averaged ICF $g_T^{(2)}(q,\tau)$ measured at $\Theta = 150°$ on the sample with [BAA]/[AA] = 1.8 wt. %. The three curves are obtained by choosing different speckles, i.e, by turning the cuvette containing the sample to different positions. During the measurement of one $g_T^{(2)}(q,\tau)$ (duration ≈ 1 h), the mean scattered intensity, i.e., the time-averaged intensity $\langle I(q) \rangle_T$, is nearly constant but not necessarily equal to the ensemble-averaged intensity $\langle I(q) \rangle_E$. The curves in Fig. 5 are labeled by the value of the quantity Y defined in Eq. (16). It is obvious from Fig. 5 that the three curves are very different although they are measured on the same sample. This difference does not arise from macroscopic inhomogeneities in the sample because, if we choose completely different positions in the cuvette but with the same Y value, we find the same $g_T^{(2)}(q,\tau)$. The phenomenon of nonergodicity is most clearly demonstrated by the reduction of the zero-time amplitude of $g_T^{(2)}(q,\tau)$ or σ_I^2. The effect of the nonergodic character of the medium is most pronounced at small Y values, i.e., when $\langle I(q) \rangle_T \gg \langle I(q) \rangle_E$. As a first analysis of the data, we determine the initial slope and amplitude of the curve obtained by plotting $\ln[g_T^{(2)}(q,\tau)-1]$ against $q^2\tau$ (cumulant analysis). Referring to Eq. (21), we thus obtain the mean-square intensity fluctuation σ_I^2 and the apparent diffusion coefficient D_A. From Eq. (19) we then
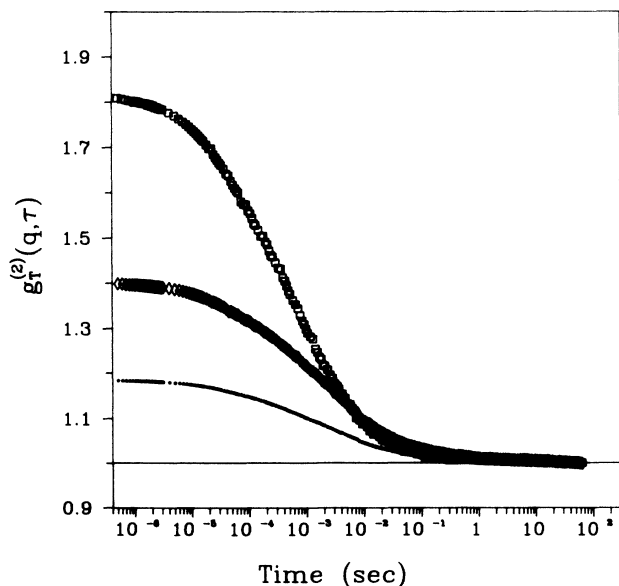
calculate $f(q, \infty)$, and using Eq. (22) we find the (short-time) diffusion coefficient D. The results of this analysis for the curves in Fig. 5 are given in Table I. We see from the results in Table I that, although the apparent diffusion coefficient D_A shows a pronounced dependence on Y, the correctly calculated diffusion coefficient D is independent of Y. It clearly shows that large values of D_A that would have been obtained in a classical analysis do not imply rapid particle motions but result simply from an incorrect analysis of the data. With respect to the results for $f(q, \infty)$, we see that it is slightly higher for the data with $Y = 3.50$. This tendency is observed in most of the data; i.e., for large Y values, the calculated $f(q, \infty)$ tends to be higher when compared with the data obtained at $Y \leq 1$. A possible explanation for this effect is the presence of residual scattering arising from dust or multiple scattering. We will discuss this later in some detail. The finite value of $f(q, \infty)$ clearly shows that there are frozen-in fluctuations in these systems that can be thought to arise from the constraints imposed on the diffusion of the particles by the gel network.

In Fig. 6 we have plotted the results for D_A and D obtained by the analysis described above for a series of measurements on a gel system with particles. The parameter Y varies, whereas the scattering angle is 90° for all experiments. As one observes, while there is hardly any dependence of D on Y, the apparent diffusion coefficient D_A shows a strong Y dependence and, furthermore, is many times larger than the true diffusion coefficient D. In Fig. 7 we have plotted the results for D_A and D obtained by the analysis described above for a series of measurements in which the parameter Y is approximately 1, whereas the scattering angle is varied between 30° and 150°. As is evident, there is hardly any dependence of D on q as one would expect for short-time self-diffusion.[13] The diffusion coefficient plotted in Fig. 7 is corrected for gel scattering (see Sec. IV B).

We now use Eq. (17) to calculate the full dynamic structure factor from the data given in Fig. 5. For the mean-square intensity fluctuation σ_I^2, we use the values found from the cumulant analysis (see Table I), and the results are plotted in Fig. 8. It can be seen in this figure that for short times all the curves fall on top of each other, which is consistent with the results obtained for the initial decay by the cumulant analysis (see results for D in Table I). One may also notice that the curve obtained from the data with $Y = 3.50$ has a higher value for $\tau \to \infty$, which is consistent with the results from Table I.

We conclude this section by giving some results obtained by performing a tedious experiment for getting the

FIG. 5. Normalized intensity correlation functions $g_T^{(2)}(q,\tau)$ for the gel with [BAA]/[AA] = 1.8 wt. %. Data taken at $\Theta = 150°$ for three different scattering volumes: squares, $Y = 3.50$; diamonds, $Y = 1.03$; dots, $Y = 0.46$. The solid line indicates the normalized baseline.

TABLE I. Mean-square intensity fluctuation σ_I^2 [Eq. (18)] and the apparent diffusion coefficient D_A for the ICF's from Fig. 5. Calculated $f(q, \infty)$ and short-time diffusion coefficient D. D_A and D are given in units of 10^{-12} m²/sec.

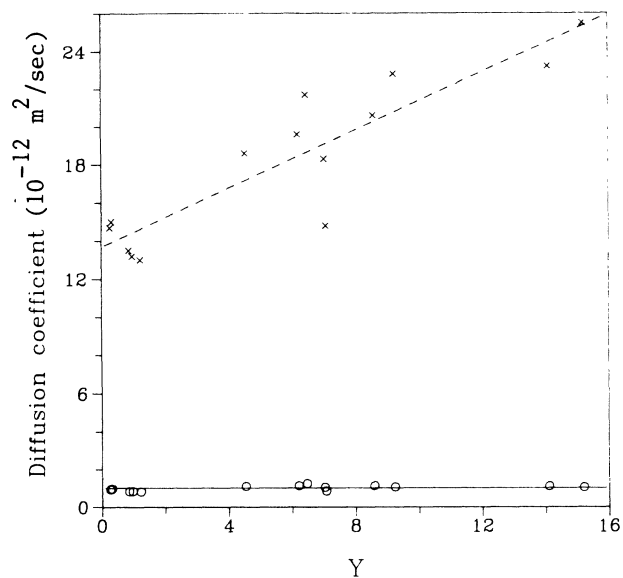| Y	σ_I^2	D_A	$f(q, \infty)$	D
3.50	0.81	6.0	0.84	1.4
1.03	0.40	4.2	0.78	1.6
0.46	0.18	3.8	0.79	1.5

FIG. 6. Apparent diffusion coefficient D_A (crosses) and calculated diffusion coefficient D (circles) against Y. Experiments at $\Theta = 90°$ for a gel ([BAA]/[AA]=4 wt. %) containing latex particles. The solid line indicates the average for D.

FIG. 8. Full dynamic structure factors calculated from the results given in Fig. 5 by using Eq. (17). Curves are labeled by the same symbols as in Fig. 5.

ensemble-averaged ICF. This experiment was done by collecting about 300 ICF's, each of duration 1 min, and by choosing a different speckle for each function. Data are taken at $\Theta = 90°$. Given these data, one has two options: either to take the average of the individually normalized ICF's denoted by $\langle g_T^{(2)}(q,\tau)\rangle_E$ or to add the unnormalized ICF's and perform a normalization with the
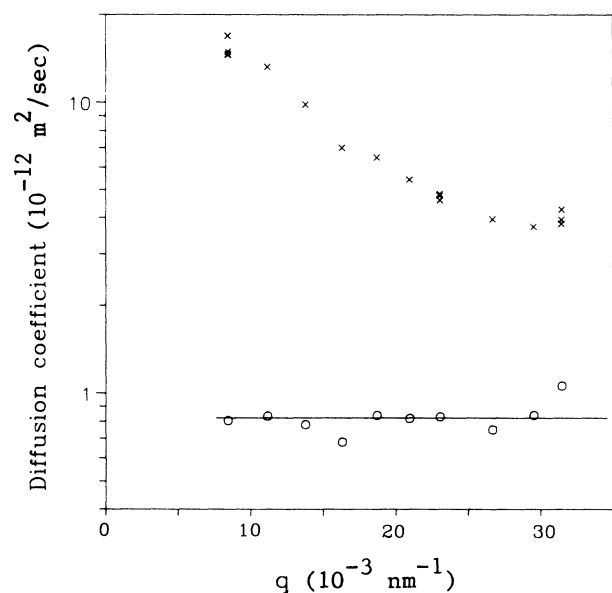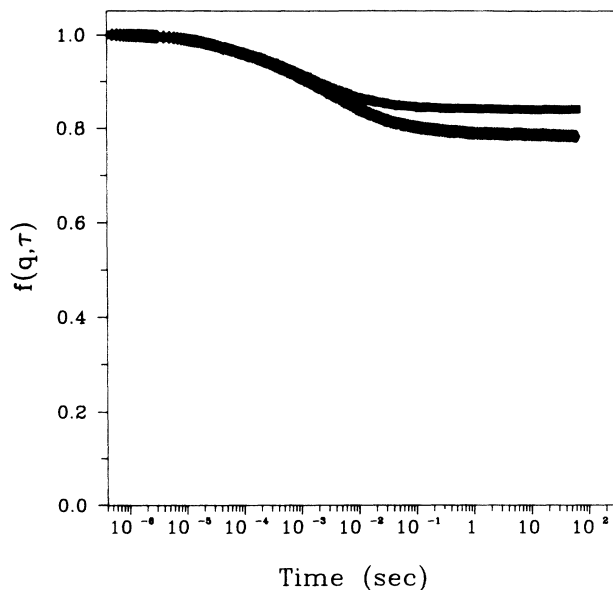
total number of counts. The latter procedure results in an estimate of the ensemble-averaged ICF $g_E^{(2)}(q,\tau)$. In Fig. 9 we have plotted the results of the two averaging procedures. One observes from the upper curve in Fig. 9 $[g_E^{(2)}(q,\tau)]$ that the amplitude at $\tau \to 0$ nearly equals that of a fully ergodic system like the dilute latex dispersion. Of course, in the limit of infinite number of measure-
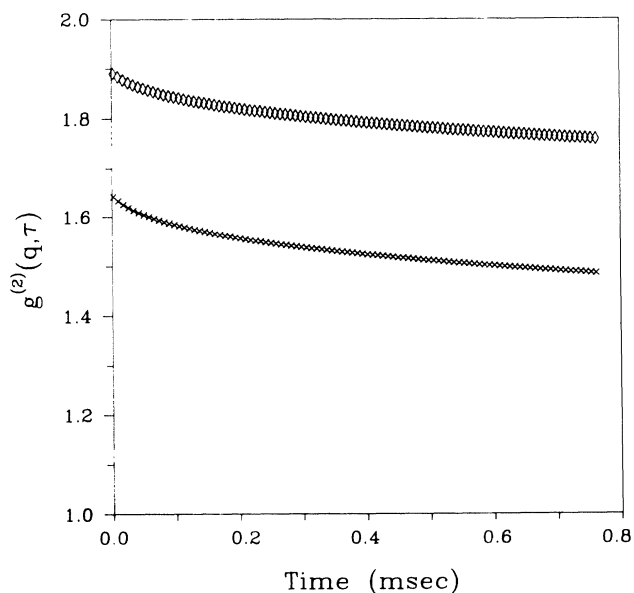

FIG. 7. Apparent diffusion coefficient D_A (crosses) and calculated diffusion coefficient D (circles) against scattering vector q. In all the experiments, Y equals approximately 1. Gel with [BAA]/[AA]=1.8 wt. % containing latex particles. The solid line indicates the average for D which is corrected for gel scattering (see Sec. VI B).

FIG. 9. Results for ensemble-averaged intensity correlation functions obtained at $\Theta = 90°$ from a gel sample ([BAA]/[AA]=1.5 wt. %). The upper curve is $g_E^{(2)}(q,\tau)$, as obtained by adding 300 unnormalized ICF's followed by a normalization. The lower curve results from an averaging of the normalized time-averaged correlation functions leading to $\langle g_T^{(2)}(q,\tau)\rangle_E$.

ments, this should be the case, but apparently 300 measurements suffice in this case to give a reasonable estimate. The function $g_E^{(2)}(q,\tau)$ can be analyzed by means of Eq. (1) resulting in a short-time diffusion coefficient (first cumulant) of 1.0×10^{-12} m²/sec. We analyze the function $\langle g_T^{(2)}(q,\tau) \rangle_E$ by using a result derived in Ref. 14. It is found there that the short-time expansion of this function is given by

$$\langle g_T^{(2)}(q,\tau) \rangle_E - 1 \approx (1-f)/f[(1+f)F-1] - 2Dq^2\tau F ,$$

$$(24)$$

where $f = f(q, \infty)$, $F = \exp[(1-f)/f]E_1[(1-f)/f]/f$, and E_1 is the exponential integral.[19] Using (24) we find that $D = 0.9 \times 10^{-12}$ m²/sec and $f(q, \infty) = 0.61$. Finally, we compare these results with those obtained from an analysis of a time-averaged ICF measured on the same gel and at the same scattering angle (the analysis is the same as the one used for the data in Table I). We then find that $D = 1.1 \times 10^{-12}$ m²/sec and $f(q, \infty) = 0.59$. It is clear that the results of these three methods agree very well. Bear in mind, however, that measuring the time-averaged ICF takes about 10 min and that collecting the data for the ensemble-averaged ICF takes about 6 h!

We will now compare the full dynamic structure factors $f(q,\tau)$ as obtained from $g_E^{(2)}(q,\tau)$ (upper curve in Fig. 9) and from the time-averaged ICF $g_T^{(2)}(q,\tau)$ (not shown here). Figure 10 gives the results. As discussed above, the experiments are performed with a coherence factor $\beta = 0.958$, whereas the theory assumes perfectly coherent detection ($\beta = 1$). Insertion of the experimental values of $g_T^{(2)}(q,\tau)$ and σ_I^2 into Eq. (18) ensures that the derived $f(q,\tau)$ has zero-time value $f(q,0) = 1$; difficulties associated with partially coherent detection in the study of nonergodic media are discussed in Ref. 14. In order to compare the two sets of data in Fig. 10, the dynamic structure factor obtained from the upper curve in Fig. 9 has been normalized to one. As one can see, there is a reasonable agreement between these curves thus supporting the theory put forward by Pusey and van Megen.[14]

Although we have presented no data here for the gels without particles, it turns out that these systems also show a similar nonergodic behavior as the systems described above. We find for these pure gels that, depending on the degree of cross-linking, the diffusion coefficient obtained from the first cumulant depends strongly on the ratio Y. Applying the same procedure as described above for analyzing ICF's, i.e., using Eq. (22), we find
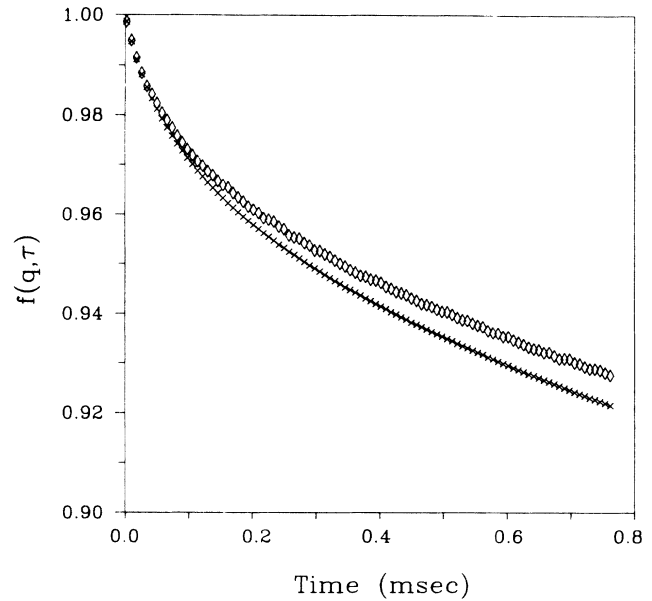

FIG. 10. Dynamic structure factor obtained from $g_E^{(2)}(q,\tau)$ by applying Eq. (1) to data of the upper curve in Fig. 9 (crosses). Also shown is $f(q,\tau)$ as obtained from a time-averaged scattering experiment and using Eq. (17) (diamonds). Note that the vertical axis ranges from 0.9 to 1.0.

diffusivities that are independent of the particular speckle under study. We also observe that these systems have frozen-in fluctuations; i.e., we find finite values for $f(q, \infty)$ (see Table II). For strong gels, this phenomenon is more pronounced than for weak gels.

IV. DISCUSSION

The main conclusion that can be drawn from the results presented in the previous section is that it is possible to extract dynamical structure factors from DLS experiments on nonergodic systems in an unambiguous way. Nonergodicity effects can cause serious problems if one neglects it by analyzing DLS experiments in the usual way, i.e., by just applying (1) (see, e.g., Table I). If one wants to avoid the tedious procedure of constructing an ensemble-averaged ICF by scanning through a nonergodic sample, one may use the theoretical results of Pusey and van Megen[14] to find from a time-averaged ICF the dynamic structure factor, which is an ensemble-averaged quantity. We now discuss some of the results in more detail.

TABLE II. Effect of gel scattering on the diffusivity of particles in the gel system with [BAA]/[AA]=4 wt. %; $f(q, \infty)$ and short-time diffusion coefficient D are calculated without correction for gel scattering. D_1 and $f_1(q, \infty)$ are values obtained for the pure gel; D_2 and $f_2(q, \infty)$ are the values for the particles with a correction for gel scattering. D, D_1, and D_2 are given in units of 10^{-12} m²/sec.

Θ	$f(q, \infty)$	D	$f_1(q, \infty)$	D_1	$f_2(q, \infty)$	D_2
30	0.984	1.1	0.710	6.8	0.998	0.9
50	0.979	1.1	0.694	7.0	0.993	0.8
70	0.972	0.8	0.674	6.5	0.987	0.6
90	0.966	1.0	0.658	7.5	0.980	0.7
120	0.953	1.0	0.640	7.9	0.971	0.7
150	0.944	1.1	0.614	7.7	0.962	0.7

A. Frozen-in fluctuations

In the paper by Nishio, Reina, and Bansil,[3] it is claimed that from DLS experiments on gels, in which polystyrene spheres are incorporated, the fraction of moving particles can be determined [in our terminology, this fraction is given by $1-f(q,\infty)$, where $f(q,\infty)$ is a measure of frozen-in fluctuations]. They used similar gel systems to those described in Sec. III with probe particles of diameter 50 and 100 nm. These authors measure σ_f^2, defined in Eq. (18), and find a value less than one, which implies partial trapping of the particles and suggests that the gel has a large interconnected space, as well as many small pores. From the q dependence of σ_f^2, a pore-size distribution is calculated. The results obtained in Ref. 3 are already discussed by Pusey and van Megen[14] in some detail; therefore here we just stress the fact that an experimental value of σ_f^2 of less than one may arise from the nonergodic character of the medium at hand, and thus all the particles may be trapped. Since the authors do not state that an ensemble-averaged ICF is constructed, such as that given in Fig. 9, it may be premature for them to draw conclusions about a fraction of moving particles. The authors notice at different positions in a sample that different results are obtained, and they attribute this to inhomogeneities inside the gel. In a sense this is correct since different scattering volumes will contain different fixed configurations $\{R_j\}$. In the framework of our present results, however, these different scattering volumes are described by different subensembles of the nonergodic medium, but all these subensembles belong to the same full ensemble. This is most clearly shown by the results in Figs. 9 and 10.

As already mentioned in the theoretical section, for a complete analysis of the scattering data, one needs a theoretical model for the dynamic structure factor $f(q,\tau)$ of nonergodic media. Since we are not aware of any such theory that is applicable to the systems at hand, we consider an assembly of independent harmonically bound Brownian particles.[14] This model has also been used to describe scattering by interacting colloidal systems[13] and polymer gels without particles.[1,20] The dynamics of harmonically bound particles were considered by Uhlenbeck and Ornstein.[21] Within the framework of this model, we envisage the gel system to be a collection of strongly scattering tracer particles in a weakly scattering medium. Noninteracting scatterers are restricted to the neighborhoods of random fixed positions $\{R_j\}$ by weak harmonic forces. For identical particles in identical environments, the dynamic structure factor for this model reads

$$f(q,\tau)=\exp\{-\Delta[1-\exp(-D_0q^2\tau/\Delta)]\} , \quad (25)$$

where $\Delta=q^2\langle\delta^2\rangle$, $\langle\delta^2\rangle$ is one Cartesian component of the long-time mean-square displacement of a particle from its average position, and D_0 is the particle's diffusion coefficient. The short-time expansion of (25) is $f(q,\tau)\approx 1-D_0q^2\tau+\cdots$, so that initially a particle diffuses as if it were free; only over longer times is the effect of the restriction imposed by the harmonic force felt. At long times we find from (25) the frozen-in component

$$f(q,\infty)=\exp(-\Delta) . \quad (26)$$

Using this model, we are able to calculate a (long-time) mean-square displacement from the experimental values of $f(q,\infty)$. In Fig. 11 we have depicted a semilog plot of $f(q,\infty)$ values against q^2 as obtained for the system with [BAA]/[AA]=1.5 wt. %. According to Eq. (26), this should give a straight line; i.e., the values for $\langle\delta^2\rangle$ found from the data should be q independent. Calculating $\langle\delta^2\rangle$ with experimental data for $f(q,\infty)$, however, shows that $\langle\delta^2\rangle$ varies systematically with q for all the systems described here; i.e., $\langle\delta^2\rangle$ appears to be larger for small q values.

Apparently, we are dealing with a distribution of mean-square displacements rather than the case where all the particles diffuse in identical environments. This is understandable in view of the fact that a network prepared by free radical copolymerization generally shows a wide distribution of linear sequences between branch points. The statistical distribution of polymer chain lengths depends on the concentrations of monomer, cross-linker, and initiator and on the radical reactivity ratios. A distribution $P(\langle\delta^2\rangle)$ of particle environments can be taken into account by generalizing Eq. (26). For identical particles but different particle environments, we then have

$$f(q,\infty)=\int_0^\infty P(\langle\delta^2\rangle)\exp(-q^2\langle\delta^2\rangle)d\langle\delta^2\rangle , \quad (27)$$

where we assume $P(\langle\delta^2\rangle)$ to be normalized to 1.

A general scheme for obtaining a displacement distribution from (27) is hampered by the fact that inversion of this equation is a well-known ill-conditioned problem.
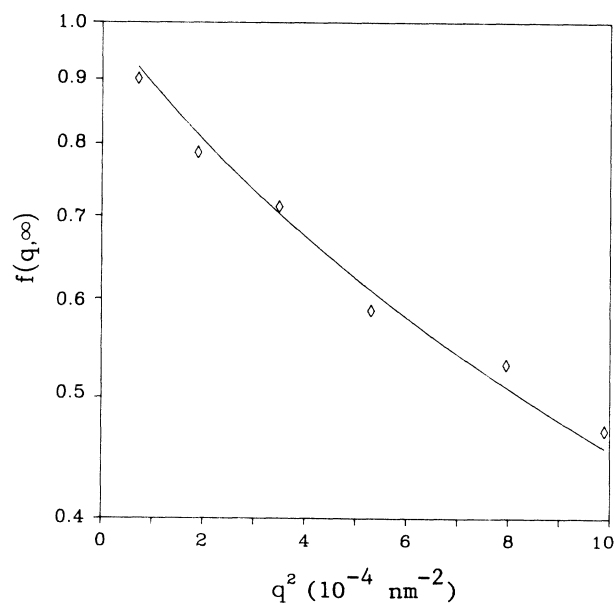

FIG. 11. Values of $f(q,\infty)$ vs q^2 for the gel ([BAA]/[AA]=1.5 wt. %) with particles. The solid line is a nonlinear least-squares fit to an exponential distribution function [Eq. (29) with $Z=0$] of particle environments. Mean rms displacement $(\langle\zeta\rangle)^{1/2}=34.7$ nm.

Rather, we assume a generalized exponential (or Schulz) distribution function and then determine its characteristic parameters. The Schulz distribution function is given by

$$P(\zeta)=(Z+1/\langle\zeta\rangle)^{Z+1}/\Gamma(Z+1)\zeta^{Z}$$

$$\times\exp[-(Z+1)\zeta/\langle\zeta\rangle]\ ,\qquad(28)$$

where $\zeta=\langle\delta^2\rangle$, $\Gamma(x)$ is the gamma function,[19] and the parameter Z is related to width of the distribution $\langle\zeta^2\rangle-\langle\zeta\rangle^2=\langle\zeta\rangle^2/(Z+1)$ (large values for Z give a sharply peaked function).

Inserting (28) in (27) gives

$$f(q,\infty)=[1+\langle\zeta\rangle q^2/(Z+1)]^{-(Z+1)}\ .\qquad(29)$$

Using this equation in a nonlinear least-squares fit to the data shows that the uncertainty in the estimated value of Z is large because of the lack of structure in the data. The analysis reveals, however, that $Z\approx0$, which means that $P(\zeta)$ reduces to an exponential distribution function. Therefore we use the exponential function for further analysis. The solid line in Fig. 11 shows the result using this exponential distribution function for data of the system with [BAA]/[AA]=1.5 wt. %. One notices a reasonable fit to the data. From the value found for the mean rms displacement, i.e., $(\langle\zeta\rangle)^{1/2}=34.7$ nm, it is obvious that the q range, which is accessible by light scattering, is too small to obtain detailed information on the distribution of displacements. A similar analysis of the data for the other systems shows that a description of $f(q,\infty)$ by means of an exponential distribution function does not work as well. We think that a reason for this is the presence of some scattering from the pure gel. In the Appendix we calculate the time-averaged ICF for the scattering that results from a sum of two nonergodic processes.

B. Effect of gel scattering

Referring to the results derived in Appendix A, we compare the results for the diffusion coefficient and $f(q,\infty)$ of the particles in the gel, with and without the gel scattering being included. From now on the subscript 1 refers to the pure gel, whereas the subscript 2 refers to the diffusion of the particles. In Table II we give results of such an analysis. These results were obtained by using Eqs. (A9) and (A10) and data from the scattering by the pure gel for the correction. ICF data obtained for the pure gel and the complete system (gel plus particles) were first treated as described in Sec. III. Again assuming an exponential distribution of environments, we find for the system given in Table II $(\langle\zeta\rangle)^{1/2}=6.2$ nm.

It is obvious from Table II that one cannot neglect gel scattering if one is interested in the diffusional motion of the particles alone. It appears that the effect of gel scattering is more important for the strong gels than for the weak gels. For example, the data given in Fig. 11 are hardly affected by a correction for gel scattering. In Fig. 12 we give results for $f_2(q,\infty)$ versus q^2 for the same system as presented in Fig. 7, where we give the diffusion coefficients corrected for gel scattering. It appears that the results for $f_2(q,\infty)$ that are corrected for gel scatter-
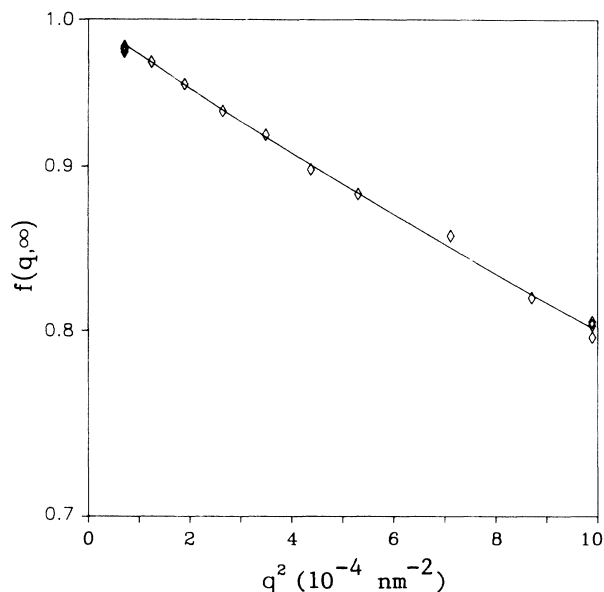

FIG. 12. Values of $f(q,\infty)$ vs q^2 for the gel ([BAA]/[AA]=1.8 wt. %) with particles. The solid line is a nonlinear least-squares fit to an exponential distribution function [Eq. (29) with $Z=0$] of particle environments. Mean rms displacement $(\langle\zeta\rangle)^{1/2}=15.8$ nm.

ing are much better described by an exponential distribution function for the particle environments than those which have not been corrected. From these results we conclude that even if the gel scattering is 40 times lower than that of the particle system, we cannot neglect it. The most obvious way to reduce effects of gel scattering is to increase the particle scattering, i.e., by increasing the tracer concentration, but in this respect one is limited because of difficulties associated with particle-particle interactions and multiple scattering. An alternative solution to this problem is to choose a polymer-solvent combination, so that the polymer is isorefractive with the solvent (index matching).

C. Effect of background scattering

Now we will discuss the possible effects on the measured ICF's due to the presence of spurious scattering. This so-called incoherent background scattering can arise from trapped dust particles or residual multiple scattering from the probes. One can expect that these effects will be most prominent when $Y\geq1$, i.e., when $\langle I\rangle_T\leq\langle I\rangle_E$. Referring to Fig. 8 and Table I, one notices that especially the value for $f(q,\infty)$, as found from the experiment where $Y=3.50$, deviates from the other two. We find similar differences for other experiments measured at $Y\geq1$. In Appendix B we give expressions for $g_T^{(2)}(q,\tau)$ which take the effect of incoherent background scattering into account. Using Eq. (B6) with $\epsilon=0.085$, we get a $f(q,\tau)$, which completely overlaps with the lower two curves in Fig. 8. From Eq. (19) we obtain $f(q,\infty)=0.79$ when σ_I and Y are replaced by $\sigma_I/(1-\epsilon)$ and $Y/(1-\epsilon)$, respectively. For D, a value of

1.5×10^{-12} m²/sec is found when this correction is applied. Thus taking spurious background scattering into account gives consistent results for $f(q,\tau)$, irrespective of the value of Y. It appears that in a series of measurements at the same scattering angle where always $Y \geq 1$, we find that the value for I_B, necessary for achieving consistent D and $f(q, \infty)$ values, is nearly constant [ϵ varies because $\langle I \rangle_T$ varies; see Eq. (B5)]. This observation gives us good confidence that, in cases where $Y \geq 1$, spurious background scattering can affect the results. Although one may correct the results, it is, however, preferable to take measurements for which $Y < 1$.

D. Summary of results

In Table III we summarize the results for the polymer systems that are described in this paper. Qualitatively, one can imagine two kinds of motion of a particle inside the gel. First, it can move relative to the gel in open spaces or "pores." Second, its motion can be strongly coupled to that of the gel. The average mean-square displacements listed in Table III represent a combination of these modes of motion, and presumably, the relative contribution of the second mode is larger in the more strongly cross-linked gels. The most striking feature of the data in Table III is that the short-time diffusion coefficient D_2 of the particles in the gels is hardly dependent on the degree of cross-linking. Apparently, the initial diffusional motion of the tracer particles in all the systems occurs in much the same aqueous environment where the particles "feel" the same (micro)viscosity. Comparing the diffusion coefficient of the particles in water with that of the particles in gels, we find a reduction of approximately a factor of five, which can perhaps be explained by the presence of dangling polymer chains, which increase the local viscosity, and by hydrodynamic interaction.[13] It is also interesting to note that the diffusion coefficient of the particles in the un-cross-linked polymer solution (at the same polymer concentration as the gel) is only about a factor of two larger than that in the gels. Although we cannot exclude the presence of chemical-bond formation between probes and polymer chains, this effect seems to be absent as shown by Allain, Drifford, and Gauthier-Manuel[2] and Nishio, Reina, and Bansil.[3]

E. Pure gel systems

To conclude Sec. IV, we will briefly discuss the results that were obtained for the pure gel systems. As already

TABLE III. Summary of short-time diffusion coefficients, mean rms displacements of tracer particles in the polymer and gel solutions. The total monomer content ([BAA]+[AA]) in all the samples is 2.5 wt. %.

[BAA]/[AA] (wt. %)	D_2 (10^{-12} m²/sec)	$(\langle \zeta \rangle)^{1/2}$ (nm)
0.0	1.3	"∞"
1.5	0.9	35
1.8	0.8	15
4.0	0.7	6

mentioned before, we find reduced initial amplitudes of the ICF's (see, e.g., Table II) implying the presence of measurable frozen-in fluctuations in these systems also. These observations are intriguing, especially in view of the on-going discussion on the discrepancies between the DLS results obtained by different groups in the field. Munch, Candau, and Hild[22] discuss some of the discordant experimental results that are related to the functional form of the measured correlation functions. These authors find exponential decay curves, whereas, e.g., Wun and Carlson[20] have found nonexponential correlation functions of the scattered light. The continuum model developed by Tanaka, Hocker, and Benedek[23] predicts exponential ICF's, whereas the model used by Wun and Carlson[20] is based on a harmonically bound Brownian particle; this leads to nonexponential correlation functions [see Eqs. (25) and (26)]. The dispute in the literature also concerns whether DLS experiments on gels have to be interpreted in the homodyne or heterodyne scheme.[11] Many workers in the field (see, e.g., Ref. 24), following the initial work of Tanaka, Hocker, and Benedek[23] use the homodyne scheme apparently without encountering serious problems associated with nonergodicity, such as reduced intercepts σ_I^2 or high apparent diffusion coefficients D_A. Tanaka, Hocker, and Benedek assumed that the scattered field is a zero-mean Gaussian variable. We have shown, however, while this assumption is valid in the full ensemble, that it is not valid for a subensemble (=scattering volume) studied in a single light-scattering experiment. Other workers (see, e.g., Refs. 22 and 25) use the heterodyne approach. The argument for using the heterodyne scheme is based on the notion that structural defects and macroscopic inhomogeneities within the gels scatter light strongly and that this elastically scattered light acts as a local oscillator which beats with light scattered from network fluctuations. We have shown, however, that the static component in the scattered light intensity, when sampled over the full ensemble, is a zero-mean Gaussian variable, and therefore an intrinsic property of the gel. Neglecting this constant component of the scattered light, one deals only with part of the system, i.e., taking only the fast fluctuating processes into account. When using the heterodyne scheme in a single time-averaged measurement, one does not take into account the frozen-in component, $f(q, \infty)$, in the dynamic structure factor. We emphasize that, to obtain the diffusivity of the gel from the apparent diffusion coefficient D_A, it is necessary to take both static and dynamic contributions properly into account. Also, in our opinion a full theoretical description of the dynamics of gels should include fluctuating as well as frozen-in states. It is interesting to mention that we can describe the dynamic structure factors, obtained for the gels, very well by the model of a harmonically bound particle.[26]

F. Concluding remarks

We have shown that the study of the diffusional motion of particles in constraining matrices, such as cross-linked gels, requires special precautions when DLS is used to determine the diffusivity. The nonergodic character of

these systems leads to experimental ICF's that are different from ensemble-averaged ICF's, and this needs special consideration. We anticipate that use of DLS in similar systems, such as those undergoing a sol-gel transition[27,28] or those used for experiments on relaxation processes in amorphous polymers,[29] will probably require an approach such as the one we have presented here. Preliminary experiments carried out in our laboratory on microemulsion gels, such as described by Capitana et al.[30] show nonergodic behavior and can be treated by the procedure used in this paper. We emphasize that a direct indication of nonergodic behavior is the observation of a reduced initial amplitude of the time-averaged ICF when compared with the value of this quantity as measured for a fully fluctuating medium. To apply the data analysis described in this paper, it is also a *conditio sine qua non* to adjust the detection optics so that the coherence factor β, given in Eq. (1), is as close as possible to 1 for an ergodic system.

We finish this section by a philosophical remark taken from the paper by Palmer:[31] "It is quite clear that the concept of thermal equilibrium depends crucially on the observational time scale which itself determines the meaning of 'fast' and 'slow.'" Or in the words by Feynman,[32] ". . . in thermal equilibrium all the fast things have happened and all the slow things not." We should bear in mind these remarks when considering experiments and theory on "ergodic" media.

Note added. Since completing this paper we have discovered one other relevant reference: Kobayasi[33] has proposed a method for collecting light-scattering data on gels by measuring (in our terminology) $\langle I(q)\rangle_T$ at various positions in the scattering cell and then calculating

$$\sigma_{\mathrm{SD}}/\langle I(q)\rangle_E$$

$$\equiv \left[\sum_{j=1}^{M} [\langle I_j(q)\rangle_T - \langle I(q)\rangle_E]^2/M \right]^{1/2} \bigg/ \langle I(q)\rangle_E .$$

Now, using Eqs. (23) and (13), we can easily show that

the estimator for the normalized variance $\sigma_{\mathrm{SD}}/\langle I(q)\rangle_E$ equals

$$\sigma_{\mathrm{SD}}/\langle I(q)\rangle_E \equiv \{\langle I^2\rangle_T - \langle I\rangle_T^2\}^{1/2}/\langle I\rangle_E = f(q,\infty) ,$$

which shows that Kobayasi's procedure is an alternative for determining $f(q,\infty)$.

ACKNOWLEDGMENTS

APPENDIX A: SUM OF TWO NONERGODIC PROCESSES

We now present results for the time-averaged intensity correlation function resulting from a medium in which a sum of two uncoupled nonergodic processes are operative. The theoretical expressions will be used for estimating the contribution of gel scattering to the scattering by a system of gel and particles.

Analogously to Eq. (10), the total scattered field is now written as

$$E(q,\tau) = E_{F,1}(q,\tau) + E_{C,1}(q) + E_{F,2}(q,\tau) + E_{C,2}(q) , \quad \text{(A1)}$$

where the subscripts F and C have the same meaning as in Eq. (10), and 1 and 2 refer to the two processes.

The total time-averaged scattered intensity reads

$$\begin{aligned} \langle I(q)\rangle_T &= \langle |E(q,\tau)|^2\rangle_T \\ &= \langle I_{F,1}(q)\rangle_T + I_{C,1}(q) + \langle I_{F,2}(q)\rangle_T \\ &\quad + I_{C,2}(q) + 2\,\mathrm{Re}(E_{C,1}E_{C,2}^*) , \end{aligned} \quad \text{(A2)}$$

where Re( ) denotes the real part, and the asterisk denotes the means complex conjugate.

The time-averaged statistical properties of the fluctuating component $E_F(q,\tau)$ of the field scattered by a particular volume of the sample is given by

$$\begin{aligned} \langle E_F(q,0)E_F^*(q,\tau)\rangle_T &= \langle E_{F,1}(q,0)E_{F,1}^*(q,\tau)\rangle_T + \langle E_{F,2}(q,0)E_{F,2}^*(q,\tau)\rangle_T \\ &= \langle I_1(q)\rangle_E[f_1(q,\tau) - f_1(q,\infty)] + \langle I_2(q)\rangle_E[f_2(q,\tau) - f_2(q,\infty)] , \end{aligned} \quad \text{(A3)}$$

where the two processes are supposed to be uncoupled.

In (A3), $f_1(q,\tau)$ and $f_2(q,\tau)$ are the dynamic structure factors associated with the scattering process 1 and 2, respectively.

For the total constant component of the scattered intensity I_C, we find

$$I_C(q) = \langle I(q)\rangle_T - \langle I_1(q)\rangle_E[1 - f_1(q,\infty)] + \langle I_2(q)\rangle_E[1 - f_2(q,\infty)] . \quad \text{(A4)}$$

Calculation of the normalized time-averaged ICF associated with the field (A1) is now accomplished by a similar procedure as the one leading to Eq. (15). After some calculation, we find

$$\begin{aligned} g_T^2(q,\tau) &= \langle I(q,0)I(q,\tau)\rangle_1/\langle I(q,0)\rangle_T^2 \\ &= 1 + Y_1^2[f_1^2(q,\tau) - f_1^2(q,\infty)] + Y_2^2[f_2^2(q,\tau) - f_2^2(q,\infty)] \\ &\quad + 2(1 - Y_1 - Y_2)\{Y_1[f_1(q,\tau) - f_1(q,\infty)] + Y_2[f_2(q,\tau) - f_2(q,\infty)]\} \\ &\quad + 2Y_1 Y_2[f_1(q,\tau)f_2(q,\tau) - f_1(q,\infty)f_2(q,\infty)] . \end{aligned} \quad \text{(A5)}$$

where

$$Y_1 = \langle I_1(q) \rangle_E / \langle I(q) \rangle_T ,$$

$$Y_2 = \langle I_2(q) \rangle_E / \langle I(q) \rangle_T . \qquad (A6)$$

One notices from (A5) that this equation reduces to Eq. (15) for one nonergodic process, because then either Y_1 or Y_2 vanishes. The limiting behavior for a fully fluctuating medium also follows from (A5) because we have to realize that, for this case, $Y_1 + Y_2 = 1$ and $f_1(q, \infty) = f_2(q, \infty) = 0$ and thus

$$g_E^{(2)}(q, \tau) = 1 + [Y_1 f_1(q, \tau) + Y_2 f_2(q, \tau)]^2 , \qquad (A7)$$

which is the correct result for an ergodic medium.

The intermediate case, i.e., one of the processes being ergodic and the other being nonergodic, also follows from (A5).

Equation (A5) can be used for gel systems because, from experiments on the pure gel (without particles), one obtains $\langle I_1(q) \rangle_E$ and $f_1(q, \tau)$, and then, by leaving the experimental conditions unchanged, one can use these results for finding $\langle I_2(q) \rangle_E$ and $f_2(q, \tau)$ from measurements on the system with the tracer particles incorporated.

For the analysis of the data we need a cumulant expansion of $g_T^{(2)}(q, \tau)$ which will be expressed as in Eq. (21). We take a short-time expansion of the dynamic structure factors $f_1(q, \tau)$ and $f_2(q, \tau)$ as in Eq. (20):

$$f_1(q, \tau) \approx 1 - D_1 q^2 \tau + \cdots ,$$

$$f_2(q, \tau) \approx 1 - D_2 q^2 \tau + \cdots , \qquad (A8)$$

where $D_1(q)$ and $D_2(q)$ are the diffusion coefficients associated with the two diffusion processes.

Substitution of (A8) into (A5) leads to a similar equation as Eq. (21), where now D_A again is an apparent diffusion coefficient given by

$$D_A = (D_1 Y_1 + D_2 Y_2) / \sigma_I^2 , \qquad (A9)$$

and the frozen-in component $f_2(q, \infty)$ appears to be

$$f_2(q, \infty) = 1 - \{ 1 - Y_1 [1 - f_1(q, \infty)] - (1 - \sigma_I^2)^{1/2} \} / Y_2 . \qquad (A10)$$

In Eqs. (A9) and (A10), σ_I^2 [defined in Eq. (18)] and D_A are determined from the time-averaged ICF measured from the system in which both processes are simultaneously operative. Equation (A5) can be solved for $f_2(q, \tau)$ and then be used to calculate this quantity from the experimentally measured $g_T^{(2)}(q, \tau)$ and the values found for Y_1, Y_2, σ_I^2, and $f_1(q, \tau)$. The solution for $f_2(q, \tau)$ is

$$f_2(q, \tau) = 1 - \{ 1 - Y_1 [1 - f_1(q, \tau)] - [g_T^{(2)}(q, \tau) - \sigma_I^2]^{1/2} \} / Y_2 . \qquad (A11)$$

APPENDIX B: INCOHERENT BACKGROUND SCATTERING

To conclude this Appendix, we give the equations for the time-averaged ICF if next to the scattering from a nonergodic medium an incoherent background is also present. This background can be though to arise from dust particles or residual multiple scattering. The scattered field for this case is given by

$$E(q, \tau) = E_F(q, \tau) + E_C(q) + E_B(\tau) , \qquad (B1)$$

where E_B is the q-independent background field.

For the total time-averaged scattered intensity, we now have

$$\langle I(q) \rangle_T = \langle I_F(q) \rangle + I_C(q) + I_B . \qquad (B2)$$

We find the time-averaged intensity correlation function by first realizing that from (B2)

$$I_C(q) = \langle I(q) \rangle_T - I_B - \langle I_F(q) \rangle_T ,$$

$$= \langle I(q) \rangle_T - I_B - \langle I(q) \rangle_E [1 - f(q, \infty)] , \qquad (B3)$$

where the second line follows from Eq. (13).

Inserting (B3) in Eq. (14) now leads to the normalized time-averaged ICF:

$$g_T^{(2)}(q, \tau) = 1 + Y^2 [f^2(q, \tau) - f^2(q, \infty)]$$

$$+ 2Y(1 - Y - \epsilon)[f(q, \tau) - f(q, \infty)] , \qquad (B4)$$

where

$$\epsilon = I_B / \langle I(q) \rangle_T . \qquad (B5)$$

Calculating now the cumulant expansion of $g_T^{(2)}(q, \tau)$, we find a similar expression for D_A, as given in Eq. (22), but with σ_I and Y replaced by $\sigma_I / (1 - \epsilon)$ and $Y / (1 - \epsilon)$. Also in Eq. (19), we have to renormalize σ_I and Y by $(1 - \epsilon)$.

To find $f(q, \tau)$, Eq. (B4) is solved, and the solution is

$$f(q, \tau) = 1 - (1 - \epsilon) / Y$$

$$+ (1 - \epsilon)$$

$$\times \{ 1 + [g_T^{(2)}(q, \tau) - \sigma_I^2 - 1] / (1 - \epsilon)^2 \}^{1/2} / Y , \qquad (B6)$$

where we have used the modified Eq. (19) for $f(q, \infty)$.

[1]F. D. Carlson and A. B. Fraser, J. Mol. Biol. **89**, 273 (1974).

[2]C. Allain, M. Drifford, and B. Gauthier-Manuel, Polym. Commun. **27**, 177 (1986).

[3]I. Nishio, J. C. Reina, and R. Bansil, Phys. Rev. Lett. **59**, 684 (1987).

[4]C. F. Schmidt, M. Bärmann, G. Isenberg, and E. Sackmann, Macromolecules **22**, 3638 (1989).

[5]P. N. Pusey and W. van Megen, Phys. Rev. Lett. **59**, 2083 (1987).

[6]D. Langevin and F. Rondelez, Polymer **19**, 875 (1978).

[7]W. Brown and R. Rymden, Macromolecules **19**, 2942 (1986).

[8]J. Newman, N. Mroczoka, and K. L. Schick, Biopolymers **28**,

655 (1989).

[9]M. Mustafa and P. S. Russo, J. Colloid Interface Sci. **129**, 240 (1989).

[10]P. G. de Gennes, *Scaling Concepts in Polymer Physics* (Cornell University Press, Ithaca, NY, 1979).

[11]B. J. Berne and R. Pecora, *Dynamic Light Scattering* (Wiley, New York, 1976).

[12]P. N. Pusey, in *Photon Correlation Spectroscopy and Velocimetry,* edited by H. Z. Cummins and E. R. Pike (Plenum, New York, 1977).

[13]P. N. Pusey and R. J. A. Tough, in *Dynamic Light Scattering,* edited by R. Pecora (Plenum, New York, 1985).

[14]P. N. Pusey and W. van Megen, Physica A **157**, 705 (1989).

[15]D. B. Sellen, J. Polym. Sci. B Polym. Phys. Ed. **25**, 699 (1987).

[16]D. E. Koppel, J. Chem. Phys. **57**, 4814 (1972).

[17]K. Schätzel, M. Drewel, and S. Stimac, J. Mod. Opt. **35**, 711 (1988).

[18]H. C. van Hulst, *Light Scattering by Small Particles* (Wiley, New York, 1957).

[19]*Handbook of Mathematical Functions,* edited by M. Abramowitz and I. A. Stegun (Dover, New York, 1965).

[20]K. L. Wun and F. D. Carlson, Macromolecules **8**, 190 (1975).

[21]G. E. Uhlenbeck and L. S. Ornstein, Phys. Rev. **36**, 823 (1930).

[22]J. P. Munch, S. Candau, and G. J. Hild, Polym. Sci. Polym. Phys. Ed. **15**, 11 (1977).

[23]T. Tanaka, L. O. Hocker, and G. B. Benedek, J. Chem. Phys. **59**, 5151 (1973).

[24]T. Takebe, K. Nawa, S. Suehiro, and T. J. Hashimoto, J. Chem. Phys. **91**, 4360 (1989).

[25]S. Mallam, F. Horkay, A. M. Hecht, and E. Geissler, Macromolecules **22**, 3356 (1989).

[26]J. L. McCarthy, J. G. H. Joosten, and P. N. Pusey (unpublished).

[27]J. E. Martin, J. Wilcoxon, and D. Adolf, Phys. Rev. A **36**, 1803 (1987); J. E. Martin and J. Wilcoxon, Phys. Rev. Lett. **61**, 373 (1988); Phys. Rev. A **39**, 252 (1989).

[28]V. R. Kaufman, S. C. Müller, K. H. Müller, and D. Avnir, Chem. Phys. Lett. **142**, 551 (1987).

[29]G. Fytas, Macromolecules **22**, 211 (1989).

[30]D. Capitana, A. L. Segre, G. Haering, and P. L. Luisi, J. Phys. Chem. **92**, 3500 (1988).

[31]R. G. Palmer, Adv. Phys. **31**, 669 (1982).

[32]R. P. Feynman, *Statistical Mechanics* (Benjamin, Reading, 1972).

[33]S. Kobayasi, Rev. Sci. Instrum. **56**, 160 (1985).